

N. Dupré · J. Gaubicher · J. Angenault · M. Quarton

Electrochemical study of intercalated vanadyl phosphate

Received: 3 June 2003 / Accepted: 3 September 2003 / Published online: 4 November 2003
© Springer-Verlag 2003

Abstract A detailed electrochemical study of Li intercalation/deintercalation in VOPO_4 compounds with various inserted molecules (H_2O , HCOOH and CH_3COOH) is presented. For $\text{VOPO}_4 \cdot 2\text{H}_2\text{O}$, water oxidation is responsible for capacity fading. In order to improve the cyclability, the electrochemical behavior of other intercalated VOPO_4 compounds, such as $\text{VOPO}_4 \cdot \text{H}_2\text{O}$, $\text{VOPO}_4 \cdot \text{HCOOH}$ and $\text{VOPO}_4 \cdot 0.78\text{CH}_3\text{COOH}$, has been studied. For all these materials, the intercalation (deintercalation) takes place in several steps. The electrochemical study of the monohydrate indicates that the vanadium-coordinated water molecule is more stable than the second water molecule towards cycling. The highest initial specific capacity values (approximately 100 mAh/g) are obtained for the compounds with the largest interlayer space. Upon cycling, the pillaring molecules are destroyed by a high-potential oxidation process, yielding a collapse of the 2D structure and thus a loss of crystallinity. As a result, the observed specific capacity is the same for all the materials after a long cycling. This capacity is higher than the anhydrous one.

Keywords Cathode · Intercalation · Lithium batteries
Phosphate · Vanadium

Introduction

Compounds of the general formula $\text{MOXO}_4 \cdot n\text{H}_2\text{O}$ ($\text{M} = \text{Ti}, \text{V}, \text{Nb}, \text{Mo}$; $\text{X} = \text{P}, \text{S}, \text{As}$; $0 \leq n \leq 2$) show

very strong metal–oxygen bonds and consequently specific structures and properties. Among them, vanadyl phosphate is an important material that has been intensively studied because it is used as a catalyst for the synthesis of maleic anhydride from n-butane or but-2-ene [1].

The structure of $\alpha\text{-VOPO}_4$ consists of chains of distorted VO_5 pyramids connected by PO_4 tetrahedra. It presents a lamellar structure with a tetragonal framework (space group $P4/n$, $a = 6.20 \text{ \AA}$ and $c = 4.11 \text{ \AA}$ [2]). Within the $\alpha\text{-VOPO}_4 \cdot 2\text{H}_2\text{O}$ structure (tetragonal, space group $P4/nmm$, $a = 6.202 \text{ \AA}$ and $c = 7.410 \text{ \AA}$ [3]), an H_2O molecule becomes the sixth vertex of each VO_5 pyramid, leading to a distorted octahedron. This framework-bound H_2O molecule establishes a hydrogen bond with the second water molecule. Then, the mentioned hydrates have a character of layered complexes/intercalates. These compounds contain systematically some V^{IV} ions (about 2–3%) counterbalanced by protons, the presence of which has been confirmed by ESR and ^1H NMR, respectively [4, 5, 6].

Some chemical intercalations of organic molecules have been performed in VOPO_4 [7, 8, 9, 10, 11, 12, 13]. A probable structure of the prepared complexes and the way of location and anchoring of the intercalated molecules into the interlayer space were suggested. This compound has, however, rarely been considered as host material for lithium batteries despite a wide-open structure and good theoretical capacity (130 mAh/g). Previous studies [4, 14] have shown that $\alpha\text{-VOPO}_4 \cdot 2\text{H}_2\text{O}$ presents a good specific capacity (between 105 and 120 mAh/g, depending on the synthesis route) but poor cyclability: the interplanar water leads to an enhanced lithium diffusion but its oxidation above 3.9 V causes a drop of the capacity after 20 cycles and, consequently, restrains the cycling potential window to 2.8–3.9 V. In addition, several layered anhydrous phases of VOPO_4 have been investigated [4, 5, 15, 16] and show variable specific capacities and stability during cycling, depending on slight structural differences related to the occupation of the interlayer space by the vanadyl bonds.

N. Dupré · J. Gaubicher · J. Angenault · M. Quarton (✉)
Laboratoire de Cristalochimie du Solide,
Université Pierre et Marie Curie – Paris VI,
Case 176, 4 place Jussieu,
75252 Cedex 05 Paris, France
E-mail: mq@ccr.jussieu.fr
Tel.: +33-1-44275544
Fax: +33-1-44272548

The present work deals with electrochemical lithium intercalation in various inserted VOPO_4 compounds along with the improvement of the cycling performance. In this way, $\text{VOPO}_4 \cdot \text{H}_2\text{O}$, $\text{VOPO}_4 \cdot \text{HCOOH}$ and $\text{VOPO}_4 \cdot 0.78\text{CH}_3\text{COOH}$ have been synthesized and electrochemically tested. Moreover, more detailed information about the water oxidation process in hydrated VOPO_4 compounds has been obtained.

Experimental

Synthesis and characterization

$\alpha\text{-VOPO}_4 \cdot 2\text{H}_2\text{O}$ was synthesized by an aqueous route, by a simple and cheap method: the amounts of V_2O_5 (99.6%, Aldrich) and excess H_3PO_4 (85%, Carlo Erba) (molar ratio V/P=1:7.3) were mixed and heated at 100 °C overnight under reflux. The obtained suspension was filtered, washed with water and acetone and finally air-dried.

The monohydrated phase of $\alpha\text{-VOPO}_4$ was prepared by partial dehydration of $\alpha\text{-VOPO}_4 \cdot 2\text{H}_2\text{O}$ at 60 °C (heating rate 100 °C/h) for 12 h under a dry argon flow. The obtained sample was liable to quickly rehydrate, so it was stored under dry argon in a glovebox.

The compounds containing formic acid or acetic acid were synthesized by exchange of the water molecules from the dihydrate. The use of $\text{VOPO}_4 \cdot 2\text{H}_2\text{O}$ offers the advantage of a wide-open interplanar space. At first, $\text{VOPO}_4 \cdot 2\text{H}_2\text{O}$ was kept under constant stirring in formic acid for one month at room temperature. The obtained yellow product was then filtered under air and washed with acetone. The exchange of water for formic acid is reversible and depends on the sample environment. So, the material has to be kept under a dry argon atmosphere at ambient temperature. A similar synthesis route has been followed to insert acetic acid and the obtained product is a yellow powder.

The water or acid content was measured by thermogravimetric analysis (TGA) under a dry argon flow, using a Setaram 92 instrument. Structure identification as well as lattice parameters were obtained from powder X-ray diffraction (XRD) patterns using a Philips PW 1050 goniometer with Cu K_α radiation ($\lambda = 1.5418 \text{ \AA}$).

Electrochemical experiments

Electrochemical measurements were performed both in galvanostatic and potentiodynamic modes using Swagelok-type cells [18] and the MacPile system [19] with Li metal as the negative and reference electrodes. The active material was mixed with 20% acetylene black carbon (Strem Chemicals) and 5% PVDF (Aldrich) as binder. The slurry obtained by adding cyclopentanone was then deposited on an aluminum disk (surface area: 1.54 cm^2) and air-dried at ambient temperature during a few hours. Under these conditions, the loading of the active material is of the order of 15 mg. A 1 M LiClO_4 solution in ethylene carbonate/dimethylene carbonate (EC/DMC, Merck) was used as the electrolyte. The cell components were transferred into an argon atmosphere prior to the assembly process.

Concerning the experiments in potentiodynamic mode, the measured current was integrated for each potential step to obtain the accumulated charge ΔQ (Ah). The number of electrons involved in the reaction, Δx , is related to the charge ΔQ by the formula: $\Delta x = \Delta Q / (FN^H)$ where N^H is the number of moles of the host material. ΔQ divided by the size of the potential step, ΔV , gives the incremental capacity $\Delta Q / \Delta V$ (Ah/V). For each potential increment dV , the following relation can be written: $\Delta Q / \Delta V = FN^H(dx/dV)$, where dx/dV is the incremental capacity in V^{-1} .

Results and discussion

Characterization results

For the hydrated phases the amount of water molecules within the interlayer spaces was deduced from TGA and leads to the global formulae $\text{VOPO}_4 \cdot 2\text{H}_2\text{O}$ and $\text{VOPO}_4 \cdot \text{H}_2\text{O}$.

The XRD pattern for $\text{VOPO}_4 \cdot \text{H}_2\text{O}$ (Fig. 1b) matches that published by Bordes [17] and confirms the absence of the anhydrous compound (Fig. 1a) and the dihydrate (Fig. 1c). Moreover, the XRD study of $\text{VOPO}_4 \cdot 2\text{H}_2\text{O}$ with increase of temperature shows a loss of intensity of the peaks for $\text{VOPO}_4 \cdot 2\text{H}_2\text{O}$ and the peaks for $\text{VOPO}_4 \cdot \text{H}_2\text{O}$ grow when the first water molecule is exfoliated. The same phenomenon is observed for the loss of the second water molecule: the peaks for $\text{VOPO}_4 \cdot \text{H}_2\text{O}$ disappear as the peaks for VOPO_4 appear. This result confirms the existence of $\text{VOPO}_4 \cdot \text{H}_2\text{O}$ as a well-defined compound. The diffraction peaks have been indexed by the means of a tetragonal unit-cell with the following refined lattice parameters $a = 6.200(4) \text{ \AA}$ and $c = 6.256(5) \text{ \AA}$. This result confirms the strong 2D character of the VOPO_4 , $\text{VOPO}_4 \cdot \text{H}_2\text{O}$ and $\text{VOPO}_4 \cdot 2\text{H}_2\text{O}$ structures because these three compounds have the same tetragonal crystal system with the same parameter value, $a = 6.20 \text{ \AA}$, and the following c values: 4.11, 6.256 and 7.410 \AA , respectively, correlated with the number of inserted water molecules.

For the formic acid intercalated compound the DTA-TGA curves point out a two-step weight loss, respectively at 50 °C and 100 °C. The first one, of strong magnitude, accounts for the loss of one acid molecule per formula unit. The second one is very faint and could be assigned to a residue of strongly coordinated water. The amount of water present within the structure is negligible in comparison to the important formic acid proportion; the molar ratio water/formic acid is equal to 1:20. So, the obtained product will be represented as

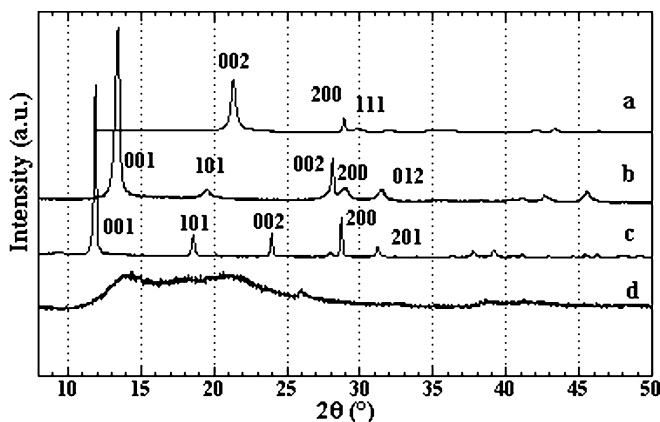


Fig. 1 X-ray powder diffraction patterns for VOPO_4 (a), $\text{VOPO}_4 \cdot \text{H}_2\text{O}$ (b), $\text{VOPO}_4 \cdot 2\text{H}_2\text{O}$ (c) and $\text{VOPO}_4 \cdot \text{H}_2\text{O}$ after 100 cycles at C/10 regime (d)

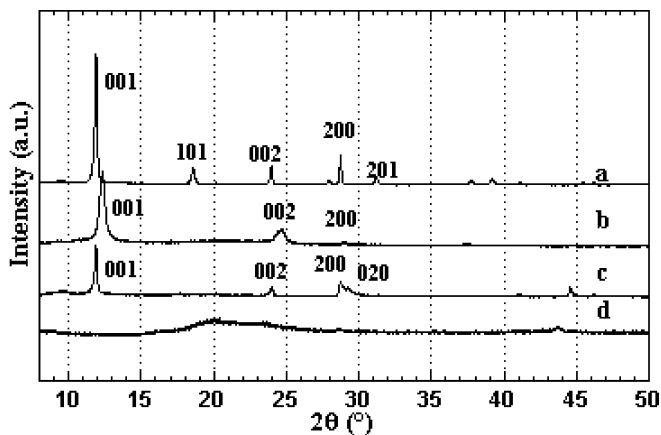


Fig. 2 X-ray powder diffraction patterns for $\text{VOPO}_4 \cdot 2\text{H}_2\text{O}$ (a), $\text{VOPO}_4 \cdot \text{HCOOH}$ (b), $\text{VOPO}_4 \cdot 0.78\text{CH}_3\text{COOH}$ (c) and $\text{VOPO}_4 \cdot \text{HCOOH}$ after 100 cycles at C/10 regime (d)

$\text{VOPO}_4 \cdot \text{HCOOH}$. The X-ray diffraction pattern (Fig. 2b) is close to that of the dihydrate (Fig. 2a). All the reflections can be indexed in the tetragonal system with the lattice parameters $a = 6.192(5)$ Å and $c = 7.238(9)$ Å. The a value indicates that no important changes have occurred within the layers themselves. The variation of the c value is correlated with the change of the “pillaring” molecule. The broadening of the l -dependent peaks is a sign for a structural disorder along the c axis. $\text{VOPO}_4 \cdot \text{HCOOH}$ is not stable under an ambient atmosphere: the sample turns green after several days while the X-ray powder diffraction pattern evolves to that of the dihydrate.

By TGA of the acetic acid intercalated sample, only one weight loss is observed, at 50 °C, equivalent to 0.78 acetic acid molecule per formula unit, leading to the formula $\text{VOPO}_4 \cdot 0.78\text{CH}_3\text{COOH}$. The X-ray diffraction study shows at least two phases (Fig. 2c), the major one being indexed by analogy with $\text{VOPO}_4 \cdot \text{HCOOH}$ in the orthorhombic system with the following lattice parameters: $a = 6.212(4)$, $b = 6.193(1)$ and $c = 7.403(5)$ Å. It should be noted that the lattice parameters determined for all intercalated samples are different from those found by Benes et al. [8] as the variations of the c parameter are not clearly correlated to the number of carbon atoms in the carboxylic acid molecule. The synthesis conditions we used were not exactly the same; therefore, the formic and acetic molecular locations and orderings could be quite different.

Electrochemical study of $\alpha\text{-VOPO}_4 \cdot \text{H}_2\text{O}$

The incremental capacity curve for the first cycle and the second reduction of the $\text{Li}/\alpha\text{-VOPO}_4 \cdot \text{H}_2\text{O}$ system, obtained in potentiodynamic mode with a typical rate of ± 10 mV/5 h, between 3.0 and 4.3 V is reported in Fig. 3. The behavior appears to be very similar to that of $\text{VOPO}_4 \cdot 2\text{H}_2\text{O}$ [4]: a succession of redox steps is observed

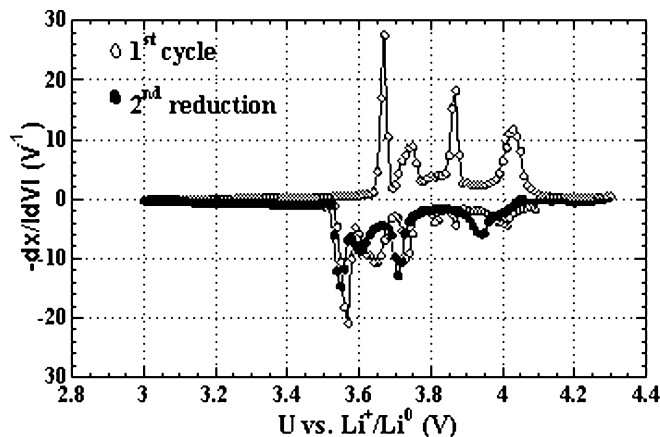


Fig. 3 Incremental capacity curves in potentiodynamic mode for $\text{VOPO}_4 \cdot \text{H}_2\text{O}$

between 3.5 and 4.1 V during the intercalation–deintercalation process, and not just a single step at 3.76 V as for the anhydrous compound [4]. The two processes observed at 3.90 and 3.85 V on the first reduction involve a very small amount of lithium and disappear on the subsequent reduction. Moreover, no corresponding peak is seen on the first oxidation. Thus, these two peaks can be considered as an indication of the formation of the material when lithium ions are first intercalated within the structure.

The reversible intercalation process occurs in four main steps and for each of them the chronoamperograms (Fig. 4) are not homothetic from one potential step to another and show variations that are typically seen for a structural transformation kinetics limited by the interface progression [20]. The two first initial chronoamperograms with monotonous decrease of the current may be related to single-phase regions of the intercalation process. On the contrary, the third and fourth transients (in Fig. 4) can be interpreted in terms of nucleation phenomena of small droplets of the new phase within the bulk of the pristine one. The increase in current with time may be related to an increase in the active surface area of the droplets. Similar behavior has

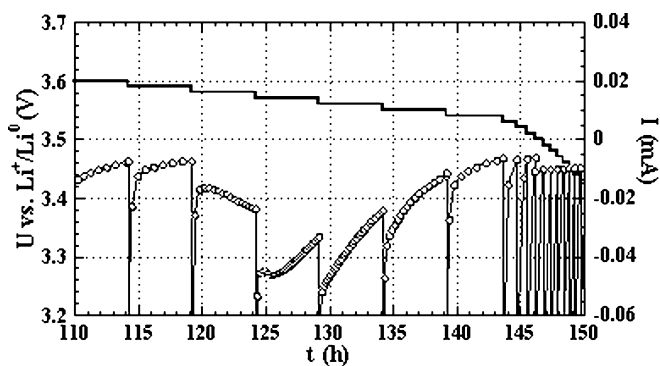


Fig. 4 Chronoamperograms corresponding to the last step of the first reduction of $\text{VOPO}_4 \cdot \text{H}_2\text{O}$

been observed during study of the cubic-to-tetragonal phase transition in $\text{Li}_x\text{Mn}_2\text{O}_4$ and has been explained using a Frumkin intercalation isotherm [21]. Although the incremental capacity peaks seem to shift from a reduction to the following one, the potentials of the corresponding structural transformation initiation appear to be the same and the change of the peak's shape indicates a decrease in the intercalation–deintercalation kinetics.

In potentiodynamic mode with a 10 mV/5 h scan step, an extracapacity phenomenon is observed at the end of the deintercalation, but it is smaller than for the dihydrate and involves only 0.06 electron per unit formula (0.30 for the dehydrate in the same conditions). This phenomenon corresponds to the interplanar water oxidation shown for the dihydrate [4, 5]. In order to test the stability of the water molecules, a cell was started on oxidation up to 4.3 V and the potential was kept at this level until the response current had reached the equivalent of a C/1000 regime (2.2 μA). Under these conditions, a weak charge variation corresponding to 0.07 electron is measured. The X-ray powder diffraction pattern obtained just after this oxidation is similar to that of the initial sample.

These results confirm the high stability of the vanadium-coordinated water molecules in comparison with the water molecules bound by hydrogen bonds in $\text{VOPO}_4\cdot 2\text{H}_2\text{O}$ [4]. For the monohydrate, the X-ray powder diffraction pattern obtained after 100 cycles shows very broad peaks, in particular in the region of the 001 peak of the anhydrous compound, indication of low crystallinity and the presence of the anhydrous phase (Fig. 1d). This suggests a disorder in the stacking of the structural planes due to successive lithium intercalations–deintercalations and the collapse of these planes due to the oxidation that occurs over a longer time frame. Thus, although the oxidation of the vanadium-coordinated water molecules is possible, the kinetics of this reaction is slower than for the weakly bonded water molecules. The vanadium-coordinated molecules are clearly more resistant towards the oxidation in terms of energy (higher departure temperature observed in TGA-DTA) and in terms of kinetics.

The electrochemical behavior of $\text{VOPO}_4\cdot\text{H}_2\text{O}$ has been studied in galvanostatic mode at different nominal regimes. The first cycles are presented in Fig. 5. The polarization (voltage difference between the reduction and oxidation curves for $x = x_{\text{max}}/2$) is, however, slightly higher than that of the dihydrate (monohydrate: 0.22 V for $\Delta x = 0.40$; dihydrate: 0.14 V for $\Delta x = 0.40$), perhaps a sign of a reduced interlayer space, the amounts of intercalated lithium being very close.

The specific capacity of the $\text{Li}/\text{VOPO}_4\cdot\text{H}_2\text{O}$ system at a C/5 (0.440 mA) regime is intermediate between those of the dihydrate and the anhydrous compound (Fig. 6). At C/10 (0.220 mA) the initial specific capacity is close to 120 mAh/g, as for the dihydrate, expressing good intercalation–deintercalation kinetics. At C/5 a smooth capacity fading is observed and after a long cycling (60

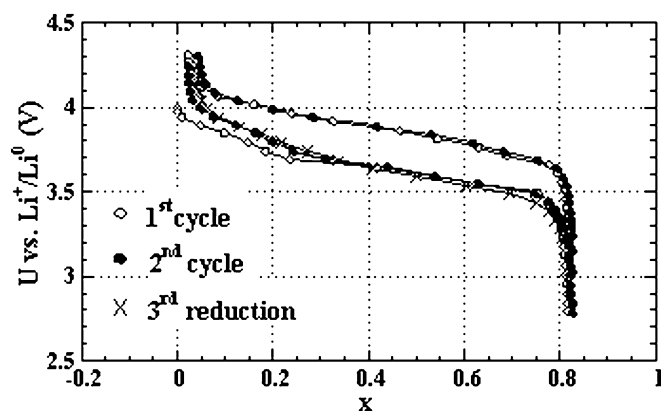


Fig. 5 Galvanostatic voltage curve for the first cycles for $\text{Li}_x\text{VOPO}_4\cdot\text{H}_2\text{O}$ at C/10 regime between 2.80 and 4.30 V

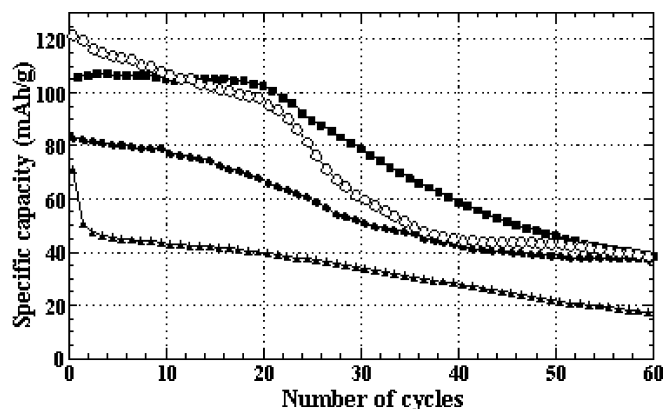


Fig. 6 Specific capacity vs. number of cycles at C/5 for VOPO_4 (filled triangles), $\text{VOPO}_4\cdot\text{H}_2\text{O}$ (filled disks), $\text{VOPO}_4\cdot 2\text{H}_2\text{O}$ (filled squares) and $\text{VOPO}_4\cdot\text{H}_2\text{O}$ at C/10 (open circles)

cycles) the specific capacities of both monohydrate and dihydrate are comparable. This result shows that the second water molecule is needed to optimize the intercalation–deintercalation kinetics. Furthermore, the extra interlayer space, in comparison to the anhydrous phase, provided by one or two water molecules seems to be directly linked to the intercalation–deintercalation kinetics and then to the cell performance for a C/5 equivalent regime.

Considering the first cycles, before the aging of the material starts to alter the performance, an increase from $c = 4.11 \text{ \AA}$ (VOPO_4) to 6.26 \AA (monohydrate) and to 7.41 \AA (dihydrate) results in an increase from 45 mAh/g (5th cycle) to 80 mAh/g and to 107 mAh/g, respectively. In the dihydrate the presence of the weakly bonded molecule, because of its easier oxidation, leads to a more drastic change in the electrochemical performance with respect to the anhydrous form, where the only factor to be taken into account is the aging of the material (i.e. loss of crystallinity). In the case of the monohydrate, the water molecules are more strongly bonded and their oxidation after several cycles yields a smoother and more progressive change in the curve for

the specific capacity versus the number of cycles. The monohydrate appears to be a compromise, so far, in between the high kinetics of the dihydrate and the relative electrochemical stability of the anhydrous form.

Other inserted molecules: formic acid, acetic acid

The reduced lifetime of the $\text{Li}/\text{VOPO}_4 \cdot 2\text{H}_2\text{O}$ and $\text{Li}/\text{VOPO}_4 \cdot \text{H}_2\text{O}$ systems, owing to the degradation of the layered structure, makes impossible any eventual application. Such a system is still able to supply a good specific capacity (about 120 mAh/g), even at a fast cycling regime. In order to maintain good crystallinity, other molecules (formic acid, acetic acid) have been inserted by water substitution, and the cycling behavior of the resulting compounds has been tested. The two criteria that have led to the choice of these “pillaring” species were their low or moderate weight (in order to keep a high massive capacity) and their larger size compared to water.

The incremental capacity curves for the $\text{Li}/\text{VOPO}_4 \cdot \text{HCOOH}$ and $\text{Li}/\text{VOPO}_4 \cdot 0.78\text{CH}_3\text{COOH}$ systems, obtained in potentiodynamic mode with a typical rate of $\pm 10 \text{ mV}/5 \text{ h}$, are reported in Fig. 7. The rate has been accelerated to $\pm 10 \text{ mV}/1.5 \text{ h}$ for $\text{Li}/\text{VOPO}_4 \cdot 0.78\text{CH}_3\text{COOH}$ under 3.70 V upon the first cycle.

For these two materials, the redox process occurs in a similar way to $\text{VOPO}_4 \cdot 2\text{H}_2\text{O}$ [4]: the reduction (oxidation)

of V^{IV} and the intercalation (deintercalation) take place in several steps. For each step, the shape of the chronoamperometric responses evidences a two-phase equilibrium with an interface progression that limits the structural transformation kinetics. Some differences can be noted, in particular concerning the incremental capacity peak positions on the second cycle. The apparent potentials, showing the beginning of each step, remain the same. The peak maxima shift can be attributed to a modification of the intercalation–deintercalation kinetics from the second cycle, without any important change within the material structure. This result is confirmed by XRD. The shift in the maxima of all intercalation peaks towards higher potentials indicates that lithium intercalation within the structure is associated with a lower energy and is probably related to the adaptation of the material towards lithium intercalation. Thus, this reaction seems to be easier in terms of energy, although the broader peaks observed for the second reduction show a lower kinetics. We have no explanation for the peak at the end of the first reduction (3.55 V).

The electrochemical behavior of the $\text{Li}/\text{VOPO}_4 \cdot 0.78\text{CH}_3\text{COOH}$ system is more complex than that of $\text{Li}/\text{VOPO}_4 \cdot \text{HCOOH}$, with an important modification between the first and second cycles (Fig. 7b), although the amount of intercalated lithium is roughly identical. Moreover, the observed incremental capacity peaks are very broad and close to each other and result in an apparent background noise. The dramatic drop of potential between 3.70 and 3.56 V is due to a change in the potential decrease rate and indicates the very slow kinetics of the system, as no response of the system is seen until a lower potential. This behavior has not been observed for $\text{VOPO}_4 \cdot 2\text{H}_2\text{O}$ and could be attributed to the presence of acetic acid molecules hindering lithium diffusion in the interlayer space, while it is possible that the first lithium intercalation modifies their ordering within the structure. The first and the second oxidations appear to be comparable, the potentials showing the beginning of each step, given by the intersection of the x-axis and the peaks initial slope, are shown to be the same. Actually, the shift of the peak maxima shows the increase in the deintercalation kinetics. This transformation can be related to a process of electrochemical formation of the material towards lithium intercalation. Other forms of VOPO_4 , like $\beta\text{-VOPO}_4$ [22], are known to undergo such a formation process, characterized by improvement of the insertion kinetics along the first electrochemical cycles.

The presence of formic or acetic acid molecules within the interlayer space induces some major differences. It appears clearly that these molecules do not simply influence the interlayer basal spacing since the potentials and the numbers of electrochemical steps vary from one system to another. Moreover, an interlayer basal spacing change may induce a potential change itself. Finally, during the electrochemical cycling, a more or less important modification of the voltammogram is

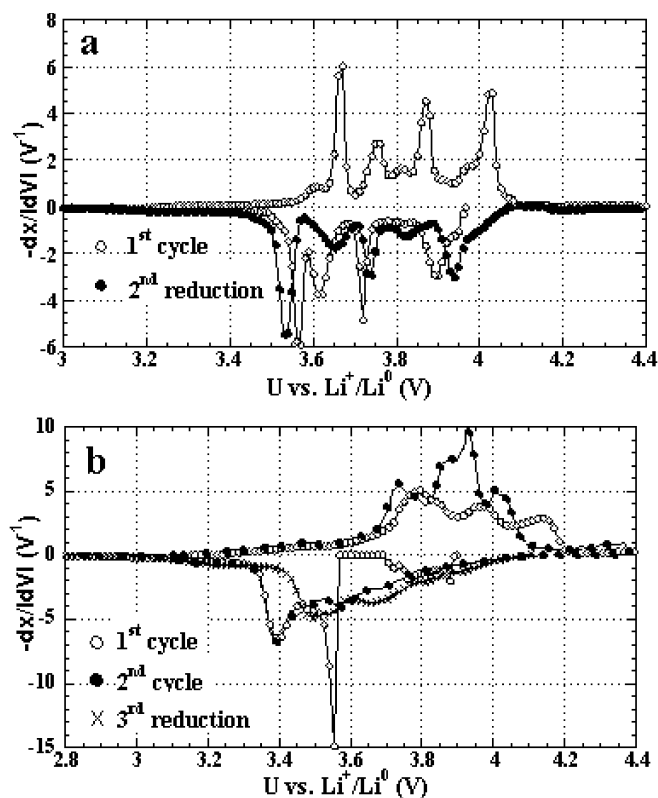


Fig. 7 Incremental capacity curves in potentiodynamic mode for $\text{VOPO}_4 \cdot \text{HCOOH}$ (a) and for $\text{VOPO}_4 \cdot 0.78\text{CH}_3\text{COOH}$ (b)

noticed that can be attributed to a kinetics modification. For small molecules like water, the first voltammograms are similar, whereas the change is more important for larger molecules, with always a decrease in the energy necessary for the intercalation–deintercalation process.

The comparison of the intercalation and deintercalation peak areas reveals extracapacity on oxidation for the two systems. Meanwhile, no extracapacity peak is associated with this phenomenon, which is rather spread out over a large potential domain. As a matter of fact, all the peaks are larger and broader on oxidation. These results show that the formic and acetic acid molecules are also oxidized upon electrochemical cycling. One may expect that the initial V^{IV} oxidation (corresponding to roughly 0.02 electron) may be also a part of this extracapacity. In order to check on this hypothesis, the Li/VOPO₄·HCOOH and Li/VOPO₄·0.78CH₃COOH systems have been oxidized up to 4.4 V until the response current has reached the equivalent of a C/1000 regime (respectively 1.92 μ A and 1.98 μ A), to measure excessive current corresponding to the extracapacity alone. Current responses corresponding with 0.98 and 0.83 electron per formula unit have been measured respectively for the Li/VOPO₄·HCOOH and Li/VOPO₄·0.78CH₃COOH systems. The oxidation of one formic or acetic acid molecule by the Kolbe mechanism [23] frees 1 electron, that is to say respectively 1 and 0.78 electron per formula unit (taking the formula into account). So, it seems that the current measured on direct oxidation and the amount of electron liberated by the “pillaring” molecule oxidation can be correlated.

The X-ray powder diffraction pattern of VOPO₄·HCOOH after cycling (Fig. 2d) does not present the 001 peaks (001 at $2\theta = 12^\circ$ and 002 at $2\theta = 25^\circ$) typical of the interlayer spacing before oxidation any longer. Meanwhile, a very broad diffusion peak is noticed from $2\theta = 18$ to 27° , that is to say in the angular zone of the anhydrous 001 reflection, whereas the $hk0$ peaks (200 at $2\theta = 29^\circ$ and 220 at $2\theta = 43^\circ$) are nearly normal. Thus, it appears clearly that the “pillaring” molecules are eliminated from within the structure, resulting in an important disorder in layer stacking. A similar structure amorphization is obtained for the Li/VOPO₄·0.78CH₃COOH system.

Therefore it appears that the vanadium-coordinated water molecule is more stable than the acid molecule within the structure and the acid molecules seem to be more stable than the weakly bonded water molecule, although they have a similar departure temperature on TGA-DTA. One may think that the criterion of stability towards oxidation is not the oxidation driving force but the bond strength with the host matrix (evaluated with the TGA-DTA departure temperature: 80 °C for the vanadium-coordinated water molecule, 50 °C for the acid molecules and the weakly bonded water molecule).

We have investigated the electrochemical behavior of the two systems in galvanostatic mode at C/10 (0.192 mA) and C/5 (0.384 mA) regimes. The potential–composition curve obtained at C/10 for the Li/VOPO₄·HCOOH

system (Fig. 8) is similar to that of the dihydrate at the same regime. The polarization is slightly higher for the material containing formic acid, a sign of a lower intercalation–deintercalation kinetics: 0.17 V for Li/VOPO₄·HCOOH; 0.12 V for Li/VOPO₄·2H₂O. The amount of intercalated lithium is furthermore higher for the dihydrate ($x_{\max} = 0.83$ compared to 0.73 here). At the end of the first cycle, a weak extracapacity is observed, which corresponds to an electron ratio equivalent to that of the dihydrate under the same conditions (0.05 electron). An oxidation start shows that, in this case, the extracapacity is much lower because it is similar to the extracapacity observed for a reduction start (0.05 electron for VOPO₄·HCOOH and 0.45 electron for VOPO₄·2H₂O). Thus it is confirmed that the molecules of formic acid are more resistant towards the oxidation process occurring at high potential, responsible for the elimination of the water from VOPO₄·2H₂O.

The study of the Li/VOPO₄·0.78CH₃COOH system reveals an extremely hindered kinetics in comparison to the two previous systems. The two first cycles (Fig. 9) are characterized by a very important polarization (the potential corresponding to the last lithium ion deintercalation is too high and out of the potential domain that can be investigated without electrolyte oxidation). A

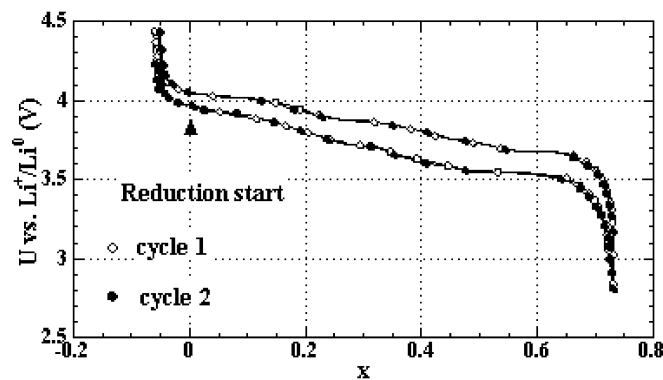


Fig. 8 Galvanostatic voltage curve for the two first cycles for VOPO₄·HCOOH at C/10 regime between 2.80 and 4.45 V

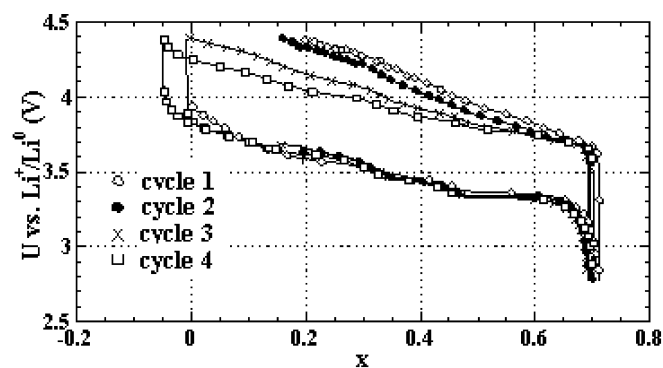


Fig. 9 Galvanostatic voltage curve for VOPO₄·0.78CH₃COOH at C/10 regime between 2.80 and 4.45 V for the first cycles

The electrochemical study of $\text{VOPO}_4 \cdot \text{H}_2\text{O}$, $\text{VOPO}_4 \cdot \text{HCOOH}$ and $\text{VOPO}_4 \cdot 0.78\text{CH}_3\text{COOH}$ has evidenced some analogies: the intercalation–deintercalation process occurs in several steps in the same potential region. It has been shown that an enhancement of the kinetics of the intercalation–deintercalation process occurs during the first cycles and is more visible for larger molecules. For small molecules like water, the first voltammograms are similar whereas the change is more important for larger molecules, with always a decrease in the energy needed for the intercalation–deintercalation process. It appears that some oxidation of the “pillar-ing” molecules occurs, which is responsible for layers’ collapse and capacity fading. Capacity fading occurs both for the hydrated compounds and for the acid inserted compounds, and is influenced by the cycling regime: a longer lifetime is observed for $\text{VOPO}_4 \cdot \text{HCOOH}$ at C/5 than for C/10. After a long cycling, all the studied materials have lost their crystallinity and the same capacity, higher than for the anhydrous compound, is observed. Thus, for all the materials the electrochemical cycling leads to the oxidation of the inserted species, amorphization and the loss of specific capacity, but the obtained structure seems to be more favorable than the anhydrous one towards lithium intercalation.

References

- Bordes E, Courtine P (1979) *J Catal* 57:236
- Bordes E, Courtine P, Pannetier G (1973) *Ann Chim* 8:105
- Tietze R (1981) *Aust J Chem* 34:2035
- Dupre N, Gaubicher J, Le Mercier T, Wallez G, Angenault J, Quarton M (2001) *Solid State Ionics* 140:209
- Dupre N (2001) Thèse Université Pierre et Marie Curie – Paris VI
- Shpeizer BG, Ouyang X, Heising JM, Clearfield A (2001) *Chem Mater* 13:2288
- Ladwig G (1980) *Z Chem* 20:70
- Benes L, Hyklova R, Kalousova J, Votinsky J (1990) *Inorg Chim Acta* 177:71
- Benes L, Votinsky J, Kalousova J, Handlir K (1990) *Inorg Chim Acta* 176:255
- Martinez-Lara M, Moreno-Real L, Jimenez-Lopez A, Bruque-Gamez S, Rodriguez-Garcia A (1986) *Mater Res Bull* 21:13
- Johnson J, Jacobson A, Brody J, Rich S (1982) *Inorg Chem* 21:3820
- Melanova K, Benes L, Zima V, Vahalova R (1999) *Chem Mater* 11:2173
- De Farias RF, Airoidi C (2002) *J Solid State Chem* 166:277
- Park NG, Kim KM, Chang SH (2001) *Electrochem Commun* 3:553
- Dupre N, Gaubicher J, Angenault J, Wallez G, Quarton M (2001) *J Power Sources* 97–98:532
- Azmi BM, Ishihara T, Nishiguchi H, Takita Y (2002) *Electrochim Acta* 48:165
- Bordes E (1987) *Catal Today* 1:499
- Guyomard D, Tarascon JM (1992) *J Electrochem Soc* 139:937
- Mouget C, Chabre Y (1996) Multichannel potentiostat galvanostat “MacPile”. Bio-Logic, Claix, France
- Chabre Y (1993) In: Bernier P, et al. (eds) *Chemical physics of intercalation*. Plenum Press, New York, p 116
- Levi MD, Gamolsky K, Aurbach D, Heider U, Oesten R (2000) *J Electrochem Soc* 147:25
- Gaubicher J, Le Mercier T, Chabre Y, Angenault J, Quarton M (1999) *J Electrochem Soc* 146:4375
- Vijk AK, Conway BE (1967) *Chem Rev* 67:623